# Prediction of Complex MR Signals of a Single Vein: Potential Advancement to Measurement of Venous Oxygen Saturation and Diameter

Sung-Hong Park[1] and Seong-Gi Kim[2,3]

[1]*Bio and Brain Engineering, Korea Advanced Institute of Science and Technology, Daejeon, Daejeon, Korea,* [2]*Radiology, University of Pittsburgh, Pittsburgh, PA, United States,* [3]*Center for Neuroscience Imaging Research, Institute for Basic Science (IBS), Dept. of Biological Sciences, SKKU, Suwon, Korea*

**Introduction :** Venous oxygen saturation level ($SvO_2$) in brain cortical regions is an important indicator of tissue oxygen consumption. Needle microelectrodes have been used to measure in vivo $SvO_2$ of cortical surface vessels as well as intracortical vessels within cortical depth < 150 μm (1), however it has been impossible to measure $SvO_2$ in a specific vein in the deeper cortical regions. MRI has a potential to measure $SvO_2$ in the deeper cortical regions non-invasively. A few methods to measure oxygen saturation levels in a single vein have been proposed (2,3), but there are limitations: the vein of interest should be parallel to the main magnetic field (2) or should be manually sub-voxel shifted to be at the center of an imaging pixel (3). In these previous methods, only phase or magnitude of MR signals inside a single vein was investigated. Here we propose a new method to measure $SvO_2$ and diameter of an intracortical vein with no limitation in physical angle and/or position, based on complex MR signal distributions using BOLD microscopy at 9.4 T.

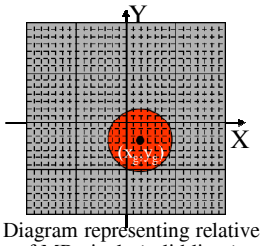


FIG. 1. Diagram representing relative locations of MR pixels (solid lines), a cross-sectional view of vein of interest (red circle), and sub-pixel gridding lines (dashed lines).

**Material and Methods :** MR signals are integration of all the spins within a pixel, therefore sub-pixel position greatly affects venous MR signals. Blood vessels were assumed to be infinitely long compared to pixel size. Finite element calculation (e.g. element width of 1/10 of the pixel width) was used (Fig. 1). The distorted position of each spin for each element was calculated based on the readout gradient strength and the angle between the blood vessel and the readout direction. The final MR complex pixel signals were calculated as a function of 4 variables, $SvO_2$, diameter (r), location of the vein ($x_g$ and $y_g$), based on the infinitely long cylinder model (4) and steady state signal intensity of GRE sequence as follows.

$$\Delta\phi_{in} = -\gamma\cdot\frac{\Delta\chi}{2}\cdot\left(\cos^2\theta-\frac{1}{3}\right)\cdot B_0\cdot TE \quad [1],$$

$$\Delta\phi_{ex} = -\gamma\cdot\left(\frac{\Delta\chi}{2}\cdot\sin^2\theta\cdot\frac{r^2}{d^2}\cdot\cos 2\phi\right)\cdot B_0\cdot TE \quad [2],$$

$$S_{in} = \rho_v\cdot\frac{(1-\exp(-TR/T_{1v}))\cdot\sin(\alpha)}{(1-\cos(\alpha)\cdot\exp(-TR/T_{1v}))}\cdot\exp(-TE/T_{2v}) \quad [3],$$

$$S_{ex} = \rho_t\cdot\frac{(1-\exp(-TR/T_{1t}))\cdot\sin(\alpha)}{(1-\cos(\alpha)\cdot\exp(-TR/T_{1t}))}\cdot\exp(-TE/T_{2t}) \quad [4]$$

where $\theta$ is the angle between the blood vessel and main magnetic field, $r$ is the radius of the blood vessel, $d$ is the distance between a point of interest outside the vein and the center of the blood vessel, $\phi$ is the angle between $d$ and the plane defined by the main magnetic field and the blood vessel, $\Delta\chi$ is the susceptibility difference between the blood vessel and tissue which is given as $4\cdot\pi\cdot\Delta\chi_{do}\cdot Hct\cdot(1-SvO_2)$, $\Delta\chi_{do}$ is the susceptibility difference between completely deoxygenated and completely oxygenated red blood cells, $Hct$ is the hematocrit level of the venous blood, $\rho_v$ and $\rho_t$ are spin densities of venous blood and tissue respectively, and $\alpha$ is the flip angle. The MR complex pixel signals ($M_{cal}$) were calculated as sum of complex numbers of all the finite elements within each pixel shown in Fig. 1 and then compared with those from experiments ($M_{exp}$). The input variables and the target function are

$$\bar{x} = \begin{bmatrix} SvO_2 & r & x_g & y_g \end{bmatrix}^T \quad [5], \qquad Err(\bar{x}) = \sum_{i=1}^{N}\left|M_{\exp,i} - M_{cal,i}(\bar{x})\right|^2 \quad [6]$$

where $N$ and $i$ represent the number of pixels within the region of interest including the blood vessel and index for the pixels, respectively. $T_{1v}$ was fixed at ~2.3 s regardless of $SvO_2$ (5). The two unknown parameters $T_{2v}$ and $\Delta\chi$ were determined as a function of $SvO_2$ (6,7). Eventually $SvO_2$ and $r$ were determined by minimizing the target (error) function.

To test the feasibility of the approach, a polyimide tube with inner diameter 1 mm was filled with MION/saline mixtures with 3% concentration of MION and was placed and fixed within a syringe (diameter 20.4 mm) filled with saline solution. In the phantom studies, $T_1$ and $T_2$ values were fixed to measured values (463 ms and 6.5 ms, respectively), and $\Delta\chi$ and diameter were calculated through the error minimization process. The real susceptibility difference between the tube and surrounding saline solution was calculated by the method proposed by Chu et al (8).

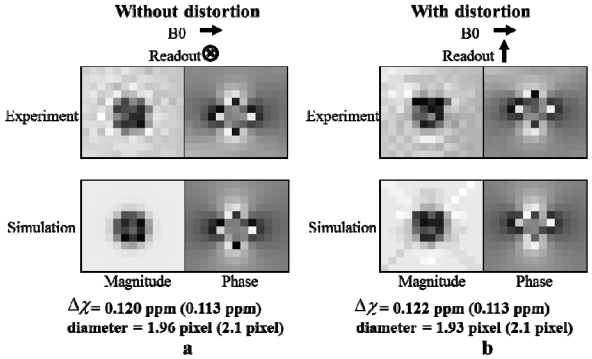


FIG. 2. **Phantom studies for susceptibility and diameter measurement**. The vessel tube was perpendicular to the main magnetic field and the readout direction was parallel (**a**) and perpendicular (**b**) to the vessel tube. All images represent a cross section of the vessel. The calculated Δχ and diameter shown on the bottom of each figure were within 10% error of the known values given within the parentheses. One pixel size is .47x.47 mm$^2$.

3D BOLD microscopy (9) was performed at 9.4T with TR = 50 ms, TE = 10 ms, and isotropic scan resolution of 0.47 mm for the phantom and with TR = 50 ms, TE = 20 ms, and isotropic voxel resolution of 86 μm for the in vivo rat brain ($N$=2). The phase signals of actual MR data were reconstructed after variations due to static field inhomogeneity were removed with a high pass filtering algorithm (10).

**Results and Discussion :** Figure 2 shows that the calculated signals from the simulation and the actual MR signals from the experiments were very similar. The susceptibility difference (between the MION dose and saline) and diameter measured from the simulations were within 10% error from their actual values (Fig. 2). Figure 3 shows the results from two intracortical veins ~1 mm apart each other at the same cortical depth of ~0.7 mm in in vivo rat brain. Visually, the signals from actual data and from simulations were very similar and measured $SvO_2$ values of the two neighboring intracortical veins were consistent, although the measured values were systematically biased compared to the values expected from literatures; the $SvO_2$ values were higher and the diameters were greater than the reported values (1,11). The $SvO_2$ values of the same intracortical veins shown in Fig. 3 from different cortical depths were also consistent with the values shown in Fig. 3. The method is new and has no restriction of physical direction and location on a vein of interest, and thus has great potentials for noninvasive measurement of venous oxygen saturation levels and diameter. Further studies are necessary to improve the measurement accuracy and reliability for in vivo studies, such as combination with a multi-echo approach.

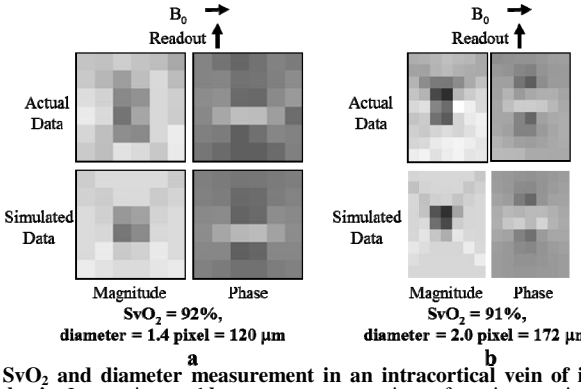


FIG. 3. **$SvO_2$ and diameter measurement in an intracortical vein of in vivo rat brain**. Images in **a** and **b** represent cross sections of two intracortical veins ~1 mm apart each other at the same cortical depth of ~0.7 mm. The calculated $SvO_2$ and diameter values are shown at the bottom of each figure.

**References** : 1. Vovenko E., Pflugers Arch 1999;437(4):617-623. 2. Haacke et al, Hum Brain Mapp 1997;5:341-347. 3. Sedlacik et al, Magn Reson Med 2007;58(5):1035-1044. 4. Reichenbach and Haacke, NMR Biomed 2001;14(7-8):453-467. 5. Tsekos et al, Magn Reson Med 1998;39(4):564-573. 6. Lee et al, Magn Reson Med 1999;42(5):919-928. 7. Weisskoff and Kiihne, Magn Reson Med 1992;24(2):375-383. 8. Chu et al, Magn Reson Med 1990;13(2):239-262. 9. Park et al, Magn Reson Med 2008;59(4):855-865. 10. Wang et al, J Magn Reson Imaging 2000;12(5):661-670. 11. Nakai et al, Stroke 1981;12(5):653-659.